ELSEVIER

Brain Research 771 (1997) 329–342

BRAIN RESEARCH

Research report

Morphological and functional characterization of an in vitro blood–brain barrier model

Kathe A. Stanness [a], Lesnick E. Westrum [a], Eleonora Fornaciari [a,c], Patrizia Mascagni [a,c], Jay A. Nelson [d], Stephan G. Stenglein [d], Tim Myers [a,b], Damir Janigro [a,b,*]

[a] *Department of Neurological Surgery, University of Washington 359914, Harborview Medical Center, 325 9th Ave., Seattle, WA 98104, USA*
[b] *Department of Environmental Health, University of Washington 359914, Harborview Medical Center, 325 9th Ave., Seattle, WA 98104, USA*
[c] *Department of Biochemistry, University of Pisa, Pisa, Italy*
[d] *Department of Molecular Microbiology and Immunology, Oregon Health Science University, L220, 3181 SW Sam Jackson Park Rd., Portland, OR 97201, USA*

Accepted 25 June 1997

Abstract

Cell culture models have been extensively used for studies of blood–brain barrier (BBB) function. However, several in vitro models fail to reproduce some, if not most, of the physiological and morphological properties of in situ brain microvascular endothelial cells. We have recently developed a dynamic, tridimensional BBB model where endothelial cells exposed to intraluminal flow form a barrier to ions and proteins following prolonged co-culturing with glia. We have further characterized this cell culture model to determine whether these barrier properties were due to expression of a BBB phenotype. Endothelial cells of human, bovine or rodent origin were used. When co-cultured with glia, intraluminally grown endothelial cells developed features similar to in vivo endothelial cells, including tight junctional contacts at interdigitating processes and a high transendothelial resistance. This in vitro BBB was characterized by the expression of an abluminal, ouabain-sensitive Na/K pump, and thus favored passage of potassium ions towards the lumen while preventing K^+ extravasation. Similarly, the in vitro BBB prevented the passage of blood–brain barrier-impermeant drugs (such as morphine, sucrose and mannitol) while allowing extraluminal accumulation of lipophylic substances such as theophylline. Finally, expression of stereo-selective transporters for Aspartate was revealed by tracer studies. We conclude that the in vitro dynamic BBB model may become an useful tool for the studies of BBB-function and for the testing of drug passage across the brain endothelial monolayer.

Keywords: Ion homeostasis; Brain microvasculature; Drug delivery; Brain tumor; Drug development; Alternative testing; Cell culture; Neurodegenerative disorder

1. Introduction

The blood–brain barrier maintains the homeostasis of the brain microenvironment, which is crucial for neuronal activity and function. Brain microvascular endothelial cells (EC) that constitute the blood–brain barrier (BBB) are responsible for the transport of metabolites, precursors and nutrients from the blood to the brain. The same cells are involved in the clearance of potassium and hydrogen ions from the brain. While blood–brain barrier EC retard the transcellular migration of most hydrophillic solutes, nutrients and sugars gain rapid access into the brain. As one may expect given the seemingly opposite properties of these BBB cells, two different subcellular mechanisms are responsible for the 'barrier' and 'transport' features of blood–brain barrier EC: tight junctions and specialized transcellular transporters, including micropinocytotic vesicles for macromolecules. The perivascular glia processes which encompass the basal lamina of the endothelial cells in the central nervous system influence the integrity of the tight junctions (or zonula occludens).

In mammals and in higher vertebrates, the sites of the blood–brain barrier are the complex tight junctions between EC that prevent the paracellular migration of hydrophillic molecules from blood to brain and vice versa [7,41]. Specialized transporters for sugars (e.g. glucose [30,37,43]) and amino acids [35] have been described in

* Corresponding author. Fax: +1 206 7318543; E-mail: ciao@u.washington.edu

blood–brain barrier EC and account for the transendothelial permeability of otherwise membrane-impermeant substances.

An often neglected aspect of the blood–brain barrier relates to its capacity to act simultaneously as a barrier and as a transporter for an ion or molecule. For example, the BBB is virtually impermeant to intraluminal potassium (K_{plasma}, [48]). However, brain (i.e. abluminal) potassium is transported to the blood by a specialized and topographically segregated Na/K-ATPase [4,51]. Thus, by combining the tight junction-mediated 'tightness' of the BBB with an asymmetric transporter, K_{CSF} remains constant in spite of K_{plasma} variations or parenchymal [K] increases resulting from neuronal activity.

Most of these specialized properties (tight junctions, micropinocytotic vesicles, transporters, ion homeostasis mechanisms) are bestowed on endothelial cells by the brain tissue [14,16,22,42,47]. Peripheral capillaries that vascularize brain tissue acquire blood–brain barrier properties [47]. Several investigators have reported that BBB-specific properties are induced in EC by neighboring astrocytes (e.g. [16,22]). Consistent with this finding, isolated blood–brain barrier EC loose their properties after culturing in vitro.

The morphological and physiological properties of the mammalian blood–brain barrier (BBB) have been characterized in detail over the years [6,8,22,23,37,42]. Due to the importance of the BBB in the understanding of central nervous system (CNS) physiology and owing to the theoretical and practical limitations of pharmacokinetic studies in vivo, it is not surprising that several attempts have been made to reproduce BBB properties in cultured cells [16,17,24,25,39,44,45,49,50]. Owing to the topographic obstacles associated with the direct investigation of brain microvessels in vivo, the structure and physiological properties of the BBB have been extensively studied in isolated microvessels and in primary cultures of brain microvascular endothelial cells [13,18,22,23,29,49]. Based on our understanding of endothelial cells in situ, an in vitro model has to reproduce all of the following properties: (1) expression of tight junctions between endothelial cells and relative lack of pinocytotic vesicles, (2) selective (and asymmetric) permeability to physiological ions, and (3) expression of blood–brain barrier-specific transporters. In addition, it is sometimes useful to immunohistochemically localize BBB markers in EC.

Advances in molecular neurobiology are bringing closer to understanding the etiology of chronic and acute degenerative brain disorders. A predictable result of the increased knowledge and awareness of CNS dysfunction mechanisms is the development of pharmaceutical strategies to treat a wide spectrum of neurological disorders, such as stroke, brain tumors, substance abuse and dementia. An equally foreseeable scenario resulting from the rapid pace of modern neuroscience is that most of the promising therapeutic approaches will fail the clinical challenge since most of the drugs acting on the CNS are effectively excluded by the blood–brain barrier. At least two approaches have been used to overcome this predicament: the development of strategies aimed at the opening of the BBB [34] or the design of substances suitable for targeted CNS delivery [5,27,38]. It is thus not surprising that several attempts have been made towards the development of an in vitro (or theoretical [45]) model of the BBB [2,17,27,38,44].

We have recently developed a new in vitro model of the BBB characterized by a tridimensional, pronectin-coated hollow fiber structure that enables co-culturing of EC with glia [21,46]. Endothelial cells in vivo are continuously exposed to shear stress generated by the flow of blood across their apical surfaces. In the hollow fiber apparatus, EC are seeded intraluminally and are exposed to flow. Under these conditions, these endothelial cells develop a morphology that closely resembles the endothelial phenotype in situ [36], demonstrating that endothelial cells grown with flow develop greater differentiation than after conventional culture. More recently, we reported the induction of BBB properties in endothelial cells grown in hollow fibers in the presence of extraluminally seeded glia; this induction of a BBB-specific phenotype included low permeability to intraluminal potassium, negligible extravasation of proteins, and the expression of a glucose transporter. In addition, culturing of EC with glia affected the overall morphology of the cells and induced the expression of BBB-specific ion channels [20,21,46].

We designed the experiments reported herein to further test the BBB nature of endothelial cells cultured with glia in hollow fibers. In particular, we wanted to answer the following questions. (1) Does the in vitro blood–brain barrier express interendothelial tight junctions; is this in vitro BBB characterized by a high transendothelial resistance? (2) Are asymmetric, ouabain-sensitive potassium transporters expressed in these cultured endothelial cells? (3) Can this in vitro model be used for pharmacological testing of the BBB permeability properties of novel drugs? Finally, we have extended our original experiments performed with bovine aortic EC and rat glioma cells by using a variety of different tissue sources, including human microvascular endothelial cells and cultures of human astrocytes.

2. Materials and methods

2.1. Cell sources

Rat brain microvascular endothelial cells (RBMEC) were isolated as previously described [18]. RBMEC were cultured in medium containing: DMEM with 1 g/l glucose (BioWhittaker), 15% plasma derived equine serum (Atlanta biologicals), 4% fetal bovine serum (HyClone), non-essential amino acids (BioWhittaker), L-glutamine 2 mM, MEM

essential vitamin mixture (BioWhittaker), Na pyruvate 1 mM (BioWhittaker), endothelial mitogen (ECGF) 10 mg/100 ml (Biomedical Technologies), heparin 5 mg/100 ml (Sigma) and PSF consisting of penicillin 100 U/ml, streptomycin 100 μg/ml, and fungizone 0.25 μg/ml (BioWhittaker).

Bovine aortic endothelial cells (BAEC) were obtained from Dr. H. Sage at the University of Washington and grown in the medium described below. C6 (a rat glial tumor line) was purchased from ATCC (Rockville, MD) and grown under the same conditions. Rat brain astrocytes (RBA) were isolated according to Refs. [19,33] with some modifications. Briefly, 21-day-old fetuses were removed from the uterus and the cortices were dissected out in cold Hanks' BSS without Ca^{2+} or Mg^{2+}. After trituration the tissue was incubated for 15 min at 37°C in a Trypsin–Hanks' mixture containing trypsin (2.5 mg/ml). After several centrifugation steps and a final trituration to break up all aggregates, the cells were filtered through a 74-μm nitex mesh and plated in flasks coated with poly-D-lysine (200 μg/flask). Cells were grown in DMEM + 10% FBS supplemented with 1.8 g/l glucose, 2 mM glutamine, 10 mM HEPES, MEM essential vitamin mixture, non-essential amino acids 100 mM each, 1 mM Na pyruvate, and PSF. After 24 h, the flasks were placed on a rotary shaker for up to 5 h to release unattached cells and microglia which were decanted and fresh medium added. This procedure was repeated every 3 days until cells reached confluence (5–10 days).

Human brain endothelial cells and human fetal astrocytes were isolated and cultured as described [31,33]. Mouse astrocytes were obtained from Dr. M. Pekny (University of Gothenburg, Sweden) and cultured as described [40].

Endothelial cells were characterized by specific uptake of Ac-LDL (DiI-Ac-LDL). For immunocytochemical staining the cells were fixed in 4% paraformaldehyde for 1 h (at 4°C). After several washes the cells were placed in a blocking buffer containing 3% goat serum, 1.5–3% BSA, and 0.1% Triton in 0.1 M TBS, pH 7.4, for 1 h to prevent non-specific binding. Primary antibodies were diluted in the same buffer and allowed to react from 1 h to overnight. MRC OX-42 antibody (Bioproducts-Harlan) and glial fibrillary acidic protein (GFAP, Dako) were used to visualize microglia and astrocytes respectively. After several washes cells were placed in a fluorescent secondary antibody (anti-mouse IgG2a for OX-42 and anti-rabbit IgG for GFAP) for 1 to 3 h.

2.2. Hollow fiber apparatus

Cells were co-cultured using hollow fiber tubes (the 'capillary vessels') inside a sealed chamber (the 'extraluminal space') accessible by ports (CELLMAX® QUAD, Cellco, Germantown, MD; see Refs. [28,36,46]). The cartridge/hollow fiber culturing system consists of artificial capillaries made from polypropylene and coated with ProNectin™ F (Protein Polymer Technologies) in a clear plastic chamber connected by gas permeable tubing to a source of growth medium allowing exchange of O_2 and CO_2. A pulsatile pump forces medium through the lumen of the artificial capillaries allowing diffusion of nutrients out to the extraluminal space (ecs) through the 0.5-μm trans-capillary pores at a controllable rate. Metabolic products are similarly removed from the cartridge. The entire apparatus resided in a water-jacketed incubator with 5% CO_2 and could be sterilely sampled by moving it inside a laminar flow hood.

EC were seeded intraluminally and allowed to establish themselves for 0 to 15 days before C6 or astrocytes were introduced into the ecs surrounding the capillaries. EC were grown to confluence in 75-cm^2 flasks, removed with trypsin and resuspended in DMEM containing 1% FBS and PSF. Amounts seeded ranged from 10×10^6 to 20×10^6 in two loadings. Flow rate was adjusted to 1 dyne/cm^2.

2.3. Morphology

2.3.1. Light microscopy

For microscopic examination, cells were fixed by intracapillary perfusion with PBS + 4% paraformaldehyde, at room temperature. Capillaries were then dissected free from the cartridge plastic support and postfixed at 4°C for 24 h. Samples were subsequently cryoprotected and frozen on dry ice. Thin (20 μm) sections were cut on sliding microtome and processed for GFAP immunoreactivity as previously described [40].

2.3.2. Electron microscopy

Capillary samples were fixed by intracapillary perfusion with 2% paraformaldehyde in a 0.1 M phosphate buffer (PB, pH = 7.2) solution. The preparations were then postfixed in the same solution in the cold for 2–7 days. Hand wafer samples (0.5 mm thick) were processed as follows: rinsed three times in 0.1 PB, post-fixed in 1% OsO_4 for 1 h, rinsed three times in PB, dehydrated through ascending grades of ethanolic alcohol solutions, infiltrated with propylene oxide and medcast resin. The samples were embedded in medcast resin and cured in a 60°C oven for 24–48 h. Semi-thin sections (1 μm) were cut in the transverse and longitudinal planes using glass knives. Ultra-thin sections (90 nm) using a diamond knife (Diatome) were made on selected blocks in both planes. Ultra-thin section were stained with uranyl acetate and lead, then viewed using a Philips 300 or 410 electron microscope.

Selected fields were photographed at instrumental magnifications of 10 000–30 000 ×. Photographic enlargements were made at 2.5 × and the prints analyzed for substructural detail.

2.4. Electrical resistance

A significant hardware modification of the existing Cellco system was performed. A metal electrode was inserted in the extraluminal space and sealed to the downstream ports by dental cement. A second electrode was placed within the inflow path for intraluminal perfusion. Thus, the extraluminal electrode (V_1) is electrically continuous with the ecs, while the luminal electrode (V_2) is immersed in the intraluminal portion of the dynamic in vitro-BBB (DIV-BBB) apparatus. The theoretical assumptions used for the development of the system to be used for trans-endothelial resistance measurements are similar to those described elsewhere [12]. Briefly, a voltage waveform is applied to V_1 and the corresponding voltage deflections are measured in V_2. The parameters we measured are the capillary resistance to current flowing perpendicular to the capillary wall, R_m (Ω/cm^2). The electrical signals collected by V_2, as well as the analog output to V_1 are delivered, acquired, timed, and analyzed by a DA/AD board interfaced to a PC.

2.5. Permeability measurements

A known concentration of the drug under investigation was dissolved directly into the media bottle and perfused intraluminally at a rate of 4 ml/min. Samples were taken from the extracapillary space or the lumen as indicated in Fig. 2. Alternatively, a concentrated bolus of the drug was injected directly into the lumen and the diffusion into the extracapillary space was monitored over time while maintaining a 4 ml/min intraluminal perfusion rate. After appropriate dilution factors were taken into account, no significant differences in the permeability values were obtained when using these different approaches. The analysis of the samples was performed by HPLC [52] (theophylline and 8-SPT) or by detection of radioactive tracers.

The permeability/surface product was calculated by graphical integration of the concentration of the drug in the lumen and in the extracapillary space over variable time periods (30–100 min). Permeability for a compound x was calculated by integrating the area under the ecs and lumen data points according to the following formula describing p (permeability):

$$\frac{K * [x]_{\text{ecs,final}} - [x]_{\text{ecs},t=0}}{\int_{0\to t} [x]_{\text{lumen}} - \int_{0\to t} [x]_{\text{ecs}}}$$

where K is a constant used to normalize rate of efflux flux for luminal surface and *lumen / ecs* volume ratios; $[x]_{\text{ecs, final}}$ and $[x]_{\text{lumen}}$ are the extracapillary space and lumen concentrations of x.

3. Results

Since the results presented in this study were obtained by using different cell types and different combinations of intraluminal and extraluminal co-cultures, we will first

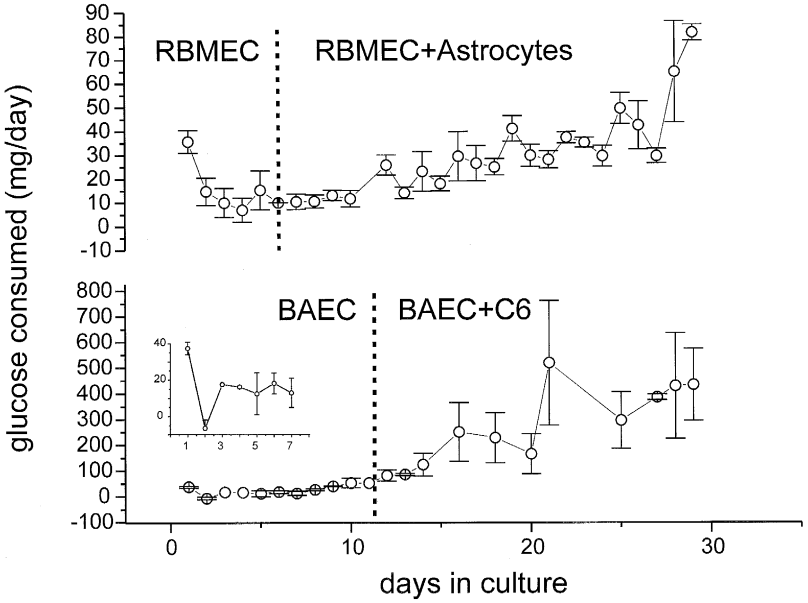

Fig. 1. Cellular growth in hollow fibers was monitored by determination of glucose consumption. Comparison of glucose consumption in RBMEC ($n = 4$) and BAEC ($n = 6$) grown adjacent to rat astrocytes and a rat glioma cell line, respectively. Note that both RBMEC and BAEC follow a typical growth pattern characterized by a high initial glucose consumption followed by a decline to a steady-state utilization. The inset shows an enlarged detail of the pattern of BAEC growth in the first week after inoculation and prior to seeding of extracapillary C6 cells. Addition of extracapillary glia (indicated by dashed lines) resulted in a progressive increase in metabolic activity. Note that rat glioma C6 cells displayed a significantly higher ($\sim 10\times$) glucose consumption.

present data dealing with the growth properties of cells seeded in the hollow fiber apparatus. A schematic representation of the latter is shown in Fig. 2. The properties of native brain endothelial cells or BAEC grown in the presence of glia are described below in separate sections dealing with measurements of potassium permeability, transendothelial electrical resistance, and passage of drugs across these endothelial monolayers.

3.1. Cellular growth in hollow fiber capillaries

Endothelial and glial cells were loaded in the hollow fiber apparatus as described in Section 2 and in Refs. [21,46]. The hollow fiber apparatus does not allow for direct evaluation of cells growth: we thus evaluated the rate of cellular growth by measurements of glucose consumption and/or lactate production (Fig. 1). In most experiments (but see Fig. 4), endothelial cells were first seeded intraluminally, followed by an inoculation of glia in the extracapillary space in the following week (ecs, see Fig. 2). We successfully cultured intraluminally bovine aortic endothelial cells, human brain microvascular endothelial cells and rat brain microvascular EC. Regardless of the source of endothelial cells, intraluminal growth in the presence of flow was characterized by an initial peak followed by a sharp decline in glucose consumption. Addition of glia caused an increase in the metabolic rate, as judged by an increase in glucose consumption (Fig. 1A). As expected, glial cells of tumoral origin (rat glioma, C6) grew at a much faster rate than primary cultures of rat brain astrocytes.

Taken together, these results demonstrated the hollow fiber apparatus can be successfully used to grow and co-culture a variety of endothelial and glial cells. The growth characteristics of glia seeded in the ecs were comparable to those observed in situ or under bidimensional conditions, inasmuch as cells of tumoral origin grew faster than their non-tumoral counterparts.

3.2. Morphological appearance of endothelial and glial cells grown in the hollow fiber apparatus

Fixed transverse sections of capillaries were obtained and cut on a cryostat. The microscopic appearance of the

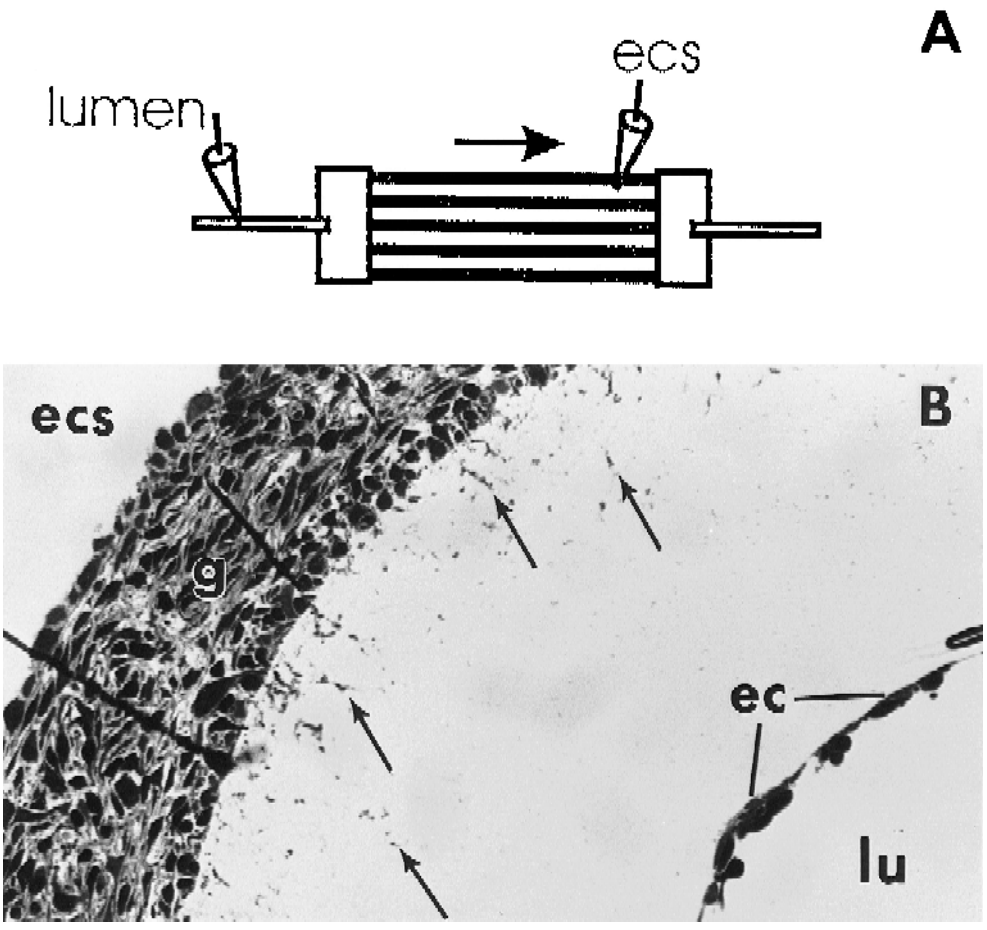

Fig. 2. A: schematic representation of the hollow fiber apparatus showing the location of the ports used to sample media and to inoculate cells. The arrow indicates the direction of flow. A photomicrograph of a transverse section of an individual capillary is shown in B. Note that the extracapillary glia grew close to the extraluminal surface and formed several cell layers. In contrast, intraluminal growth of endothelial cells is characterized by a monolayer structure. Lu, lumen; ecs, extracapillary space; ec, endothelial cells; g refers to rat glioma cells (C6).

sections revealed that intraluminally seeded endothelial cells formed a monolayer structure (Fig. 2, ec) as previously reported by Ott et al. [36]. Extraluminal glia, in contrast, developed extensive multilayer growth (ecs in Fig. 2). Interestingly, we consistently observed that glia formed cellular elongations within the capillary wall, suggesting that actual contiguity between extra- and intraluminal cells may be established.

Two cartridges were processed for electron microscopy following co-culture of BAEC and rat glioma cells and

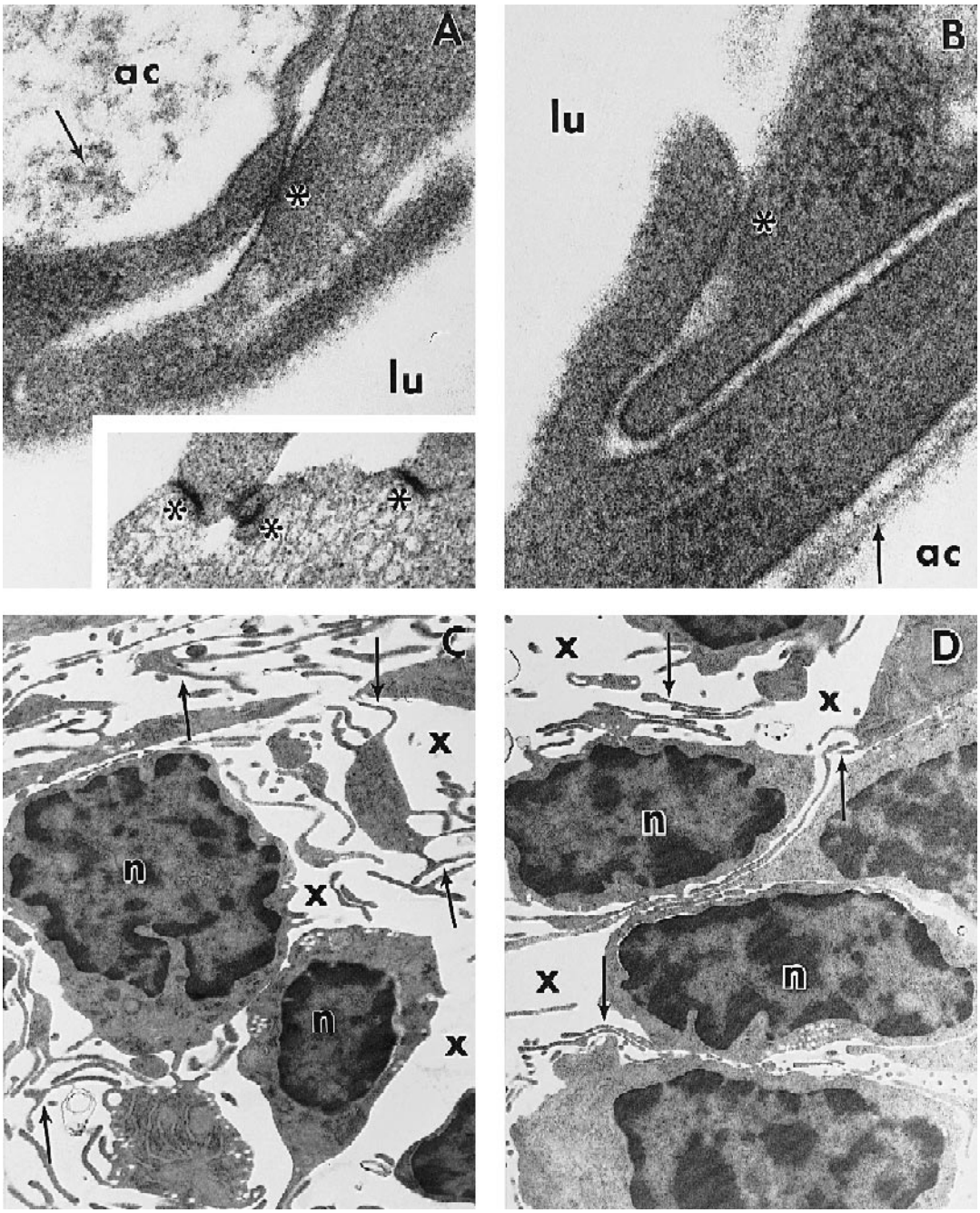

Fig. 3. Electron microscopic investigation of cellular growth in the hollow fiber apparatus. BAEC were grown in the presence of extraluminal rat glia for 21 days. At this time point, a blood–brain barrier to potassium was present (see text). A: intraluminal endothelial cells form a monolayer characterized by interdigitation of EC processes and tight junctions (asterisk). The inset shows a series of tight junctional contacts between two adjacent cells. Note the electron-dense material deposits on the artificial capillary (ac) indicated by the arrow. B: another example of intimate contact between neighboring endothelial cells. The tight junctions together with the characteristic geometry of these cell-to-cell interactions are the substrate of the barrier properties of these cells. A tight junction (zonula occludens) is indicated by the asterisk. C: in contrast to intaluminal endothelial cells, extraluminal glia do not grow in monolayer structures, nor do glia form tight junctions; thus, the observed barrier properties in hollow fibers are not due to an astrocytic barrier. Note the large extracellular spaces between cell bodies (indicated by x) and the elongations (arrows) growing into the transcapillary openings. N, nucleus. D: another example of extraluminal growth; C6 glioma cells.

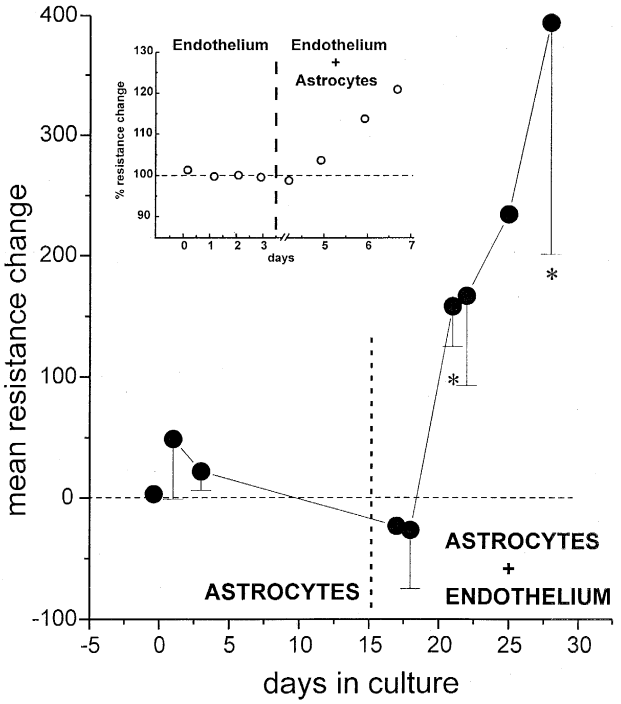

Fig. 4. Endothelial cells grown in hollow fibers with glia form a barrier characterized by high electrical resistance. Human endothelial cells were co-cultured with human fetal astrocytes, but glial cells were seeded first. Endothelial cells were added as indicated by the vertical bar. Note that the TER did not change significantly during extraluminal astrocytic growth. When EC were added intraluminally, a progressive increase of TER was observed ($n = 3$; $P < 0.05$). Initial resistance was 37.5 Ω/cm^2. Final resistance values ranged from 583 to 1100 Ω/cm^2 after 5 weeks in culture. The inset shows the results from an experiment where endothelial cells (BAEC) were grown intraluminally prior to inoculation of extraluminal astrocytes (primary culture). Note that no increase in TER was observed until the co-culture was established (each data point represents the mean of two experiments; final resistances were 721 and 838 Ω/cm^2 after 3 weeks of co-culture).

induction of a BBB to potassium (see below). Electron microscopy analysis of ultra-thin sections demonstrated the expression of several BBB endothelium-specific features, including tight junctions (indicated by asterisks in Fig. 3). These EC formed typical structures characterized by interdigitations where sometimes several contiguous tight junctions could be seen (see inset in Fig. 3A). The abluminal side of the membrane was characterized by electron-dense material, presumably reflecting the existence of a basal lamina-like structure onto the surface of the capillary (arrows in Fig. 3B). The overall 'tightness' of the endothelium lining the capillary lumen closely resembled the general structure of BBB endothelial cells.

Glial cells appeared densely packed at the light microscopic level (e.g. Fig. 2D). However, electron microscopy revealed that extraluminal growth was characterized by large cell-free gaps (stars in Fig. 3C,D). As previously noted, these glia grew elongations within the transcapillary pores (arrows).

3.3. Transendothelial electrical resistance measurements in hollow fibers

One of the most difficult blood–brain barrier characteristics to reproduce in vitro is the high electrical resistance across microvascular endothelial cells. Our previous results obtained by estimates of transendothelial potassium fluxes [46], together with the finding that intraluminal EC formed numerous tight junctions (see above) suggested that the DIV-BBB could reproduce the high electrical resistance estimated for in situ BBB EC [11,12]. To this end we developed an 'on-line' electrical resistance measurement

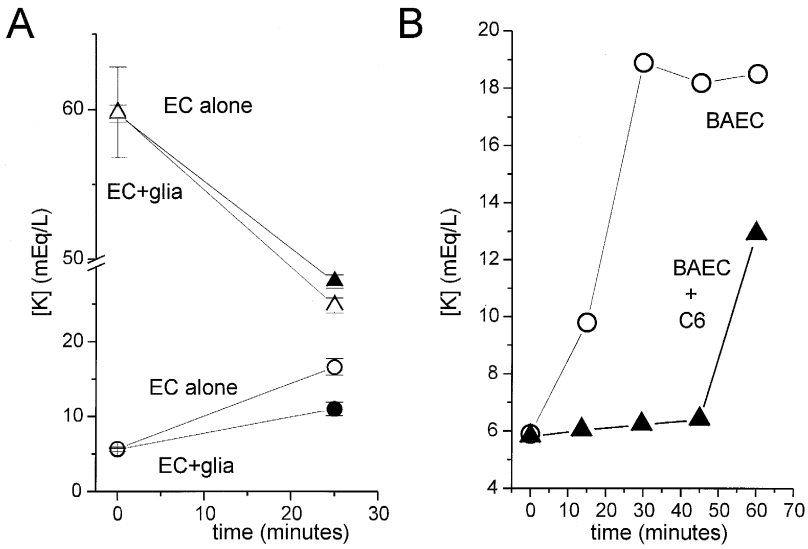

Fig. 5. Asymmetry of the in vitro BBB: potassium fluxes from the intraluminal to the extraluminal space are prevented, while efflux in the opposite direction is possible. High potassium concentrations were added either extraluminally (A) or intraluminally (B) and $[K]_{ecs}$ (triangles) and $[K]_{lumen}$ (circles) levels were monitored over time. The rate of potassium efflux was the same in cultures of BAEC alone (open symbols) or following co-culture of EC with glia (filled symbols). B: time course of potassium accumulation (18 mM applied intraluminally) in the extracapillary space in cultures of BAEC alone (○) or BAEC + C6 (▲).

device capable of monitoring trans-endothelial resistance (TER) changes in hollow fiber-cultured endothelial monolayers grown in the presence or absence of glia.

Endothelial cells grown intraluminally in the absence of glia did not develop high TER. In three experiments (BAEC) the TER measured after 7 days of intraluminal growth was $27.5 \pm 32\ \Omega/cm^2$. Similarly, the transcapillary resistance of cultures obtained following extracapillary growth of glia alone (either C6 or human astrocytes) remained low ($> 50\ \Omega/cm^2$). Dramatic increases in TER were observed after co-culturing of extracapillary glia with intraluminal EC (e.g. Fig. 4). The inset shows the TER changes observed in a culture of BAEC + astrocytes; in this example, EC were first seeded intraluminally and allowed to grow for 4 days. Note that no significant increase in TER was observed during this period of time. When glia were added to the culture (as indicated by the vertical line), the TER values increased dramatically. After co-culturing of astrocytes and BAEC for 3–4 weeks TER values stabilized at $736 \pm 38\ \Omega/cm^2$ ($n = 4$). The inset in Fig. 4 shows the averaged data from two separate cultures; electrical resistance was measured on-line for 7 days at 1-h intervals.

To rule out that prolonged growth of extraluminal glia was responsible for the changes in TER observed, we reversed the inoculation procedure and extraluminal glia were grown for 2 weeks prior to inoculation of EC intraluminally (Fig. 4, $n = 3$). Note that no significant increase in TER was observed during the first 2 weeks of growth, and that a rapid increase in TER was achieved after introduction of EC.

3.4. Asymmetry of potassium movements across the in vitro blood–brain barrier

In our previous study [46], we demonstrated that endothelial cell co-cultured with glia in the hollow fiber apparatus develop a barrier to intraluminal potassium. We further investigated the dynamics of potassium movement across the in vitro blood–brain barrier by measuring the rate of potassium efflux from the extracapillary space (Fig. 5). Elevated concentrations of $[K]_{ecs}$ (15–60 mM) were applied while measuring $[K]_{ecs}$ and $[K]_{lumen}$ (triangles and circles, respectively). The experiments were performed prior to or following induction of blood–brain barrier properties by BAEC/C6 co-culturing. Thus, the open symbols refer to data from cartridges where only BAEC were grown, while the filled symbols refer to data from BAEC/C6 co-cultures. Note that under both experimental conditions, efflux of $[K]_{ecs}$ occurred at similar rates (1.46 ± 0.21 and 1.26 ± 0.16 mM/min in BAEC and BAEC + C6, respectively; $n = 4$). In contrast, when high concentrations of potassium were applied intraluminally, 0.11 ± 0.006 mM/min were allowed across the endothelial cell monolayer (see Fig. 5B and Ref. [46]). Passage of potassium from the ecs to the lumen depended on $[K]_{ecs}$ and

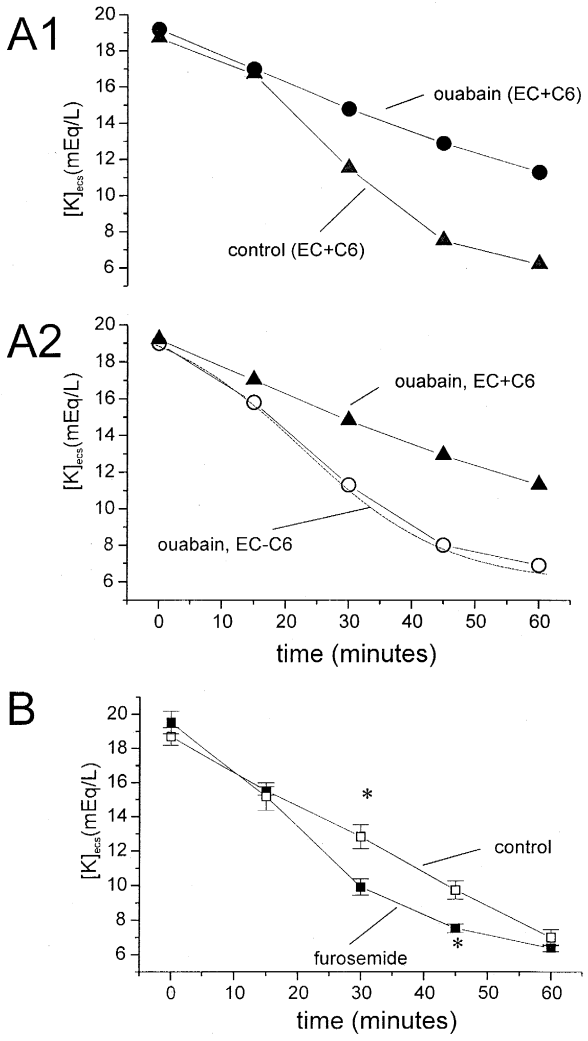

Fig. 6. Effects of ion transport inhibitors on potassium efflux from the extracapillary space. A: ouabain (at 100 μM) reduces the rate of potassium efflux following extraluminal application in a co-culture of endothelial and glial cells (A1; mean of three experiments). A2: the effects of ouabain were not observed in cultures of endothelial cells alone (open circles; the dotted line represents the time course of $[K]_{ecs}$ decay in ouabain-free media). B: in endothelial cultures, in contrast, furosemide exerted a significant ($P < 0.05$, $n = 6$) effect and $[K]_{ecs}$ clearance was increased during the first 45 min. Furosemide failed to exert any significant effect on $[K]_{ecs}$ clearance in EC/glia co-cultures.

was significantly reduced at lower $[K]_{ecs}$ (0.2 mM/min at $[K]_{ecs} = 16$ mM; 0.28 mM/min at 20 mM; 1.26 mM/min at $[K]_{ecs} = 60$ mM; $n = 3$).

The pharmacological properties of potassium efflux from the extracapillary space were investigated by preincubation of the extraluminal portion of the hollow fiber apparatus with 100 μM ouabain (Fig. 6). Ouabain significantly decreased potassium efflux in cultures where a BBB to potassium was established by prolonged (> 2 weeks) co-culturing of EC and glia. Ouabain effects were not observed in cultures with EC alone.

Further characterization of transendothelial ion fluxes in

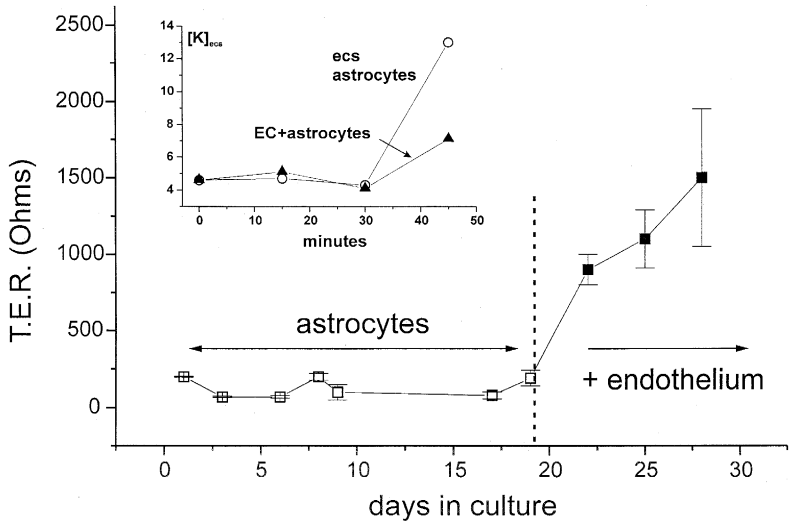

Fig. 7. Correlation of TER increases and development of a barrier to intraluminal potassium. Human astrocytes were grown in the extracapillary space prior to inoculation of intraluminal EC. Permeability to intraluminal potassium was tested prior to and following co-culture; in the inset, open circles refer to ecs potassium accumulation in glial cultures, while filled triangles report results obtained from the same cartridge, but 1 week following co-culturing with intraluminal human brain EC. In the same experiment, TER values were measured in four cartridges: note the increase in transendothelial resistance following co-culturing.

glia/endothelial co-cultures were performed by applying (intraluminally) the $K^+/Cl^-/Na^+$ co-transport inhibitor furosemide [3]. Furosemide was applied intraluminally at a concentration of 2 mM (Fig. 6B). In cultures containing only intraluminal endothelial cells, furosemide accelerated the rate of extraluminal potassium clearance from the extracapillary space (0.19 ± 0.05 mM/min in control; 0.32 ± 0.04 mM/min after furosemide; $n = 4$). This ef-

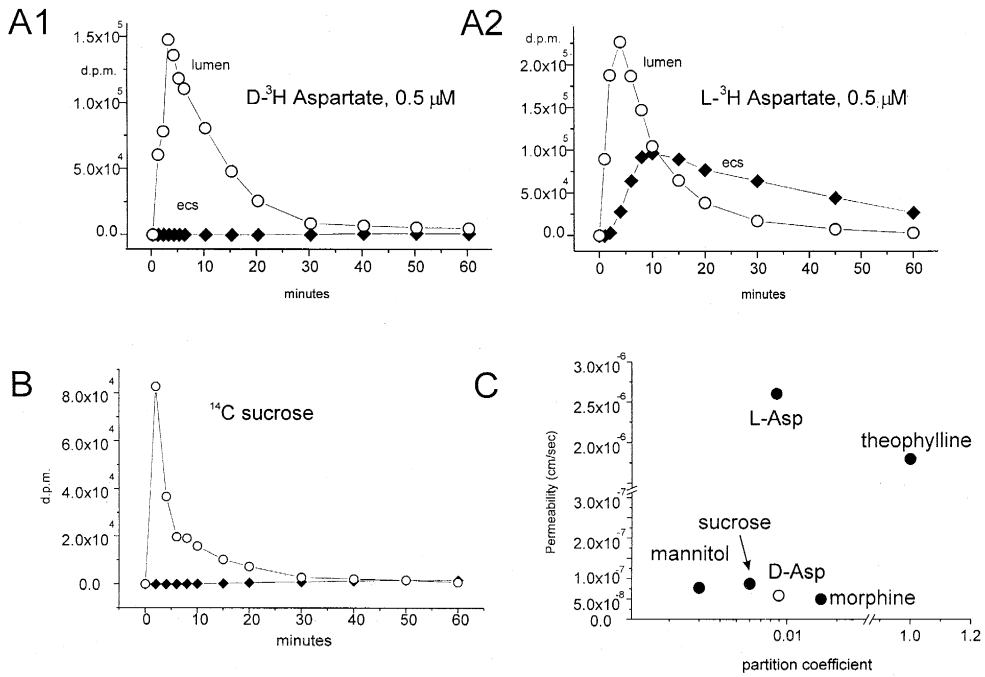

Fig. 8. Pharmacokinetic properties of the in vitro BBB. Drugs were applied intraluminally and microliter extraluminal/intraluminal amounts were sampled at the intervals indicated. A1, A2: stereospecificity of aspartate transport. Note the lack of extraluminal D-Asp accumulation in the extracapillary space and the passage of L-Asp under identical experimental conditions (same cartridge in A1 and A2). B: the BBB-impermeant molecule sucrose did not accumulate significantly in the extracapillary space following a prolonged intraluminal perfusion. C: cumulative results from the experiments performed on various substances injected in the lumen and sampled extraluminally. The permeability values were obtained by graphical integration of the signals.

fect, however, was not observed in glia/endothelial co-cultures after establishment of a BBB (0.194 ± 0.036 and 0.199 ± 0.0047 in control or furosemide, respectively).

3.5. Correlation of potassium measurements with TER

In a series of experiments, changes in intraluminal potassium permeability were compared to the development of a high transendothelial electrical resistance. To this end, cells were challenged with high intraluminal potassium (16–18 mM) while monitoring $[K]_{ecs}$. Prior to the exposure to high potassium, a reading of transcapillary resistance was taken. Fig. 7 shows the cumulative result of a typical experiment. Human endothelial cells were seeded intraluminally following extraluminal growth of human astrocytes. The permeability to $[K]_{lumen}$ in cultures containing glia but not EC was extremely high (inset); at the same time point (9 days of extraluminal growth, asterisk in Fig. 6), TER was $< 100\ \Omega/cm^2$ ($n = 4$). Following inoculation and growth of intaluminal EC, both potassium permeability and TER underwent profound changes. TER values increased progressively to $> 1000\ \Omega/cm^2$ while potassium permeability was significantly decreased.

3.6. Pharmacological studies

One of the main goals of in vitro modeling of the blood–brain barrier is to develop a system suitable for ex situ testing of transendothelial permeability. We have thus attempted to correlate in vitro BBB permeability values to the octanol: water partition coefficient. The compounds tested were injected intraluminally and sampled extraluminally prior to either radiolabel quantification (L- and D-[^{3}H]Asp; [^{14}C]sucrose; [^{14}C]mannitol; [^{3}H]morphine) or HPLC analysis (8-SPT and theophylline). The results of these experiments are shown in Fig. 8. Note that there is an excellent correlation between the oil/water partition coefficient and the tendency of the drugs to accumulate into the extracapillary space. The only significant exception to this finding was observed when comparing the permeability values of two stereoisomers of aspartic acid, L-Asp and D-Asp. While the biologically active substrate L-Asp was rapidly accumulated into the extracapillary space, the D-isomer did not show any appreciable passage from the lumen.

4. Discussion

The use of cultured vascular endothelial cells as a model of vascular permeability has been well established and has yielded to significant advancements in the understanding of microvascular physiology. However, serious limitations associated with the use of cultured brain endothelial cells has hampered the development of a reliable model of the blood–brain barrier. For example, it has been difficult to reproduce in cultured cells the high electrical resistance normally found across BBB endothelial cells in situ; furthermore, cultured brain endothelial cells lose some of their specific markers following in vitro culturing [16]. One approach used to mimic the growth environment of in vivo brain EC has been the use of glia/endothelial co-cultures [9,16,17]. Alternatively, investigators have attempted to imitate the physiological environment of microvascular endothelial cells by exposing the cells to flow [36]. We here report the characteristics of an in vitro blood–brain barrier model characterized by both intraluminal flow and co-culture of endothelial cells with glia.

The model system used for these studies results from a modification of a traditional cell culture system normally used for extensive culturing of non-EC cells. Cell culture on hollow fibers was first described by Knazek et al. [28] and has since then been extensively exploited. Ott et al. [36] used a hollow fiber cell culture apparatus for studies of flow-mediated effects on endothelial cells growth. We have further developed this system by allowing combinations of intra- and extraluminal growth to study the effects of glia on endothelial cells. The dynamic, in vitro BBB model (DIV-BBB [46]) is constituted of a plastic support containing a variable number of artificial capillaries (AC, 300 μm cross diameter with a lumen of approximately 75 μm). These capillaries bear 0.5-μm trans-capillary pores that allow free diffusion of solutes from the extraluminal compartment to the intraluminal space and vice versa. The capillaries are intraluminally perfused at various shear stress rates by pulsatile flow. In a previous study we have shown that induction of BBB-like characteristics occurs following prolonged co-culture of glia and bovine aortic endothelial cells [46]. In addition, electrophysiological investigations have shown that glia can induced the expression of BBB-specific ion channel proteins in non-BBB endothelial cells [20,21]. Several questions, however, remained unanswered following these initial studies and were addressed by the experiments described herein.

4.1. Both peripheral and CNS endothelial cells form a BBB-like structure when co-cultured with glia

We have successfully grown a variety of cells in hollow fibers, including EC of human, rodent and bovine origin. Since it is known that BBB properties of brain microvascular EC are lost following prolonged culturing in vitro, we attempted to maintain these BBB properties in culture by adding glia to the extraluminal compartments. Under these conditions, and with intraluminal flow, both non-brain and brain microvascular EC developed a high transendothelial electrical resistance, a barrier to intraluminal (but not extraluminal) potassium and a selective permeability to a variety of substances characterized by different hydrophilicity. The most parsimonious explanation for these results is that in the presence of glia, peripheral EC are induced to express BBB properties; our data also suggest

that these properties are maintained in native BBB EC in vivo (and can be preserved in vitro) by neighboring glia. Our experiments have not directly assessed whether diffusible factors or direct interaction of the two cell types are necessary, but previous studies have suggested that the latter is required [21,46].

Interestingly, the pattern of endothelial cells growth in the intraluminal portion of the hollow fibers was characterized by an initial rapid expansion followed by a quasi static growth and was independent from the source of endothelial cells. In contrast, under bidimensional 'petri dish' culturing conditions, differences between growth patterns of BAEC, human EC and rat brain microvascular cells are commonly observed. It thus appears that EC growth rate depends heavily on the presence of flow, in agreement with what previously reported by Ott et al. [36].

The data presented herein may suggest that any combination of glia and endothelial cells may prove sufficient to reproduce blood–brain barrier properties. This, however, does not seem to be true since, for example, human umbilical cord EC failed to develop blood–brain barrier properties when co-cultured with extraluminal C6 cells (not shown). Furthermore, we have recently shown that astrocytes from GFAP-deficient mice fail to induce BBB properties in BAEC (Pekny, Stanness and Janigro, submitted). Thus, while BBB properties could be induced in both peripheral and CNS endothelial cells in vitro, these phenomena are restricted to certain subpopulations of endothelia, and require co-presence of astroglia expressing the astrocyte-specific intermediate filament GFAP.

4.2. Endothelial nature of the in vitro BBB

Since co-culturing of extraluminal glia was a mandatory condition for the induction of BBB properties in our system, we performed a number of experiments to rule out that the restricted passage to ions and larger molecules was not due to a non-specific 'plugging' of transcapillary pores by glia. We thus attempted to induce a barrier to potassium by culturing glial cells in the absence of intraluminal endothelium. No restricted passage was observed under these conditions, nor did extraluminal glia significantly affect the transcapillary resistance. Similarly, electron microscopy revealed that while intraluminally grown EC formed numerous tight junction, extraluminal glia grew in a random tridimensional network and allowed for extensive extracellular space formation. Interestingly, these glia formed intracapillary extensions suggesting that an interaction between the two contiguously grown cells types may have occurred.

Due to the size of the capillary lumen, light microscopy of the endothelial cell layer appeared similar to the continuous endothelium of large precapillary vessels. However, the subcellular morphological characteristics of intraluminal endothelial growth closely resembled the pattern of cellular differentiation observed at the BBB in situ. These EC formed extensive tight junctions and grew as flat and thin (< 1 μm) monolayers. Cytoplasm vesicles were observed at a density similar to that described in vivo. Both simple and complex interdigitations were seen between neighboring cells and tight junctional densities were frequently observed. Interestingly, EC cultured on hollow fibers made a matrix that by electron microscopic analysis resembled the basement membrane of EC in vivo.

4.3. Potassium transport across the in vitro BBB

Passage of potassium ions from the blood to the brain is negligible under physiological conditions; thus, $\Delta[K]_{plasma}$ does not alter $\Delta[K]_{CSF}$ (CSF = cerebrospinal fluid). However, efflux of K^+ from the brain to the blood is possible due to the strategic abluminal location of the endothelial Na/K ATPase. Hence, excess K^+ accumulation in the brain (e.g. during epileptic seizures) can be regulated by potassium clearance into the blood [15]. While the mechanisms responsible for the blood–brain barrier properties of EC are well understood, little is known on the role that BBB EC play in clearance of potassium from the brain. Simultaneous measurements of interstitial/intraluminal [K] changes with potassium-sensitive electrodes and monitoring, in vivo, of BBB electrical resistance are extremely difficult to perform in vivo, and are confounded by a number of variables, including blood pressure changes, direct damage to the capillaries, etc. It is thus almost imperative that these studies be performed by using a simplified model in vitro.

To this end we have measured bi-directional fluxes of potassium ions across the DIV-BBB to test the hypothesis that together with tight junction/high electrical resistance expression, these EC were characterized by an asymmetric transporter for potassium ions. The presence of an extraluminal Na/K-ATPase was tested in our experiments by using both cultures of BAEC alone and co-cultures of EC and glia. Only the latter displayed an ouabain-sensitive potassium efflux, suggesting that the presence of glia directly induced this marker of BBB physiology. In contrast, we found that the expression of a luminal furosemide-sensitive transporter was inhibited by the co-culturing process. This was assessed indirectly by measuring the efflux of potassium from the extracapillary space during intraluminal application of furosemide.

We hypothesize that the accelerated efflux of $[K]_{ecs}$ following furosemide was due to a diminished reuptake of potassium from the lumen into the extracapillary space. This mechanism has been described in several endothelial cell types, but its expression in the mature mammalian blood–brain barrier is controversial [3,4]. It therefore appears that the co-culturing of glia with EC induced in the latter some of the ion transport mechanism normally exhibited at the BBB level, including the expression of cation channels [21] and an ouabain-sensitive Na/K pump. At the same time, a decreased functional expression of a trans-

porter not normally associated with blood–brain barrier function occurred.

4.4. Drug passage across the DIV-BBB

Drug and solute transport into the brain from the blood is limited by EC membrane permeability, intracellular metabolism and the lack of a major paracellular 'leak' route. Owing to the absence of transcellular 'pores' or fenestrations, extravasation of drugs into the CNS depends largely on the lipid solubility of the drug and on the presence of drug transporters. The development of new drug delivery systems to bypass the BBB, as well as the design of drugs that do not cross the blood–brain barrier depends heavily on the availability of a biological model of the blood–brain barrier that allows for a careful yet rapid quantification of drug accumulation in the CNS following systemic administration. Several investigators have developed in vitro (or mathematical [45]) models of trans-BBB drug passage [2,10,17,25,26,32,29]. One of the limitations of the available in vitro models has been the capability to simultaneously reproduce the permeability properties of EC membrane and the expression of transport systems. This is particularly important when dealing with pharmacokinetic or pharmacodistribution studies where both lipophilicity and co-transport/facilitated transport become important.

When the DIV-BBB was exposed to intraluminal substances known to permeate reluctantly through the in vivo BBB (such as morphine, sucrose or mannitol), the calculated transendothelial permeability values were consistent with those reported from in vivo studies. For example, a permeability ratio of >100 between theophylline and sucrose has been reported in vivo: similar results were obtained in the DIV-BBB ($p_{\text{theo}} = 1.88 \times 10^{-6}$ cm/s; $p_{\text{sucrose}} = 8.8 \times 10^{-8}$ cm/s). We did, however, notice that the absolute values of P derived from our study are higher than those reported in vivo. p_{morphine} in our system was 5×10^{-8} cm/s against a reported value of 5×10^{-6} [1]. This is surprising, since one would expect that the values obtained in vitro should be lower than those observed in vivo in intact animals. There are several possible explanations for this discrepancy. Firstly, the studies performed in vivo are difficult to cross reference because of the different techniques used (brain uptake, single pass, etc.) or for the different formulae used to quantify passage of a given substance into the brain. Secondly, it is known that the cerebral blood flow has a significant effect on the distribution of drugs in the CNS. In our system, flow was maintained constant throughout the experiment but it is difficult to compare the contribution of capillary flow and shear stress in vivo where the capillary diameter is of the order of a few microns to our model system (diameter >50 μm). Finally, owing to the kinetic properties of transcellular transport, it is important to remember that the time allowed for drug perfusion (or the intervals used for integration of the plasma and ecs concentrations) bears a significant effect on the values of p obtained. The values reported in Fig. 8C refer to experiments performed and analyzed in a 15-min interval following intraluminal application of the drug at 1 ml/min: we have found a strong dependency of the p-value calculated at different time intervals. Thus, after prolonged exposure the permeability to sucrose increased from 2×10^{-7} cm/s at $t = 10$ min to 5×10^{-6} cm/s at $t = 60$ min, when the p-value reached a steady state. Thus, when extrapolating data from the DIV-BBB to in vivo studies, one must keep in mind that the time of exposure to the drug may play a role in determining the absolute permeability values. The relationship between lipophilicity and permeability in the DIV-BBB was similar to that reported by others in vivo [1].

A further similarity between the selective drug permeability of the in vivo BBB and the in vitro model has been found when comparing the permeability of non-BBB permeant aminoacids that are transported across the BBB by a stereospecific transporter. We found that the biologically active L-isomer of aspartic acid was transported across the DIV-BBB at a significantly higher (>100) rate than its D-isomer counterpart. This is an important finding, because it suggests that this in vitro BBB model may be suitable for the study of permeation of drugs that are normally accumulated in the CNS in virtue of a BBB-specific transporter.

Although the currently available models of in vitro permeability resemble intact endothelial cells in several ways, it has been thus far impossible to faithfully reproduce all of the numerous properties of the in situ EC blood–brain barrier. It is thus important to delimit the scope of each individual model and define exactly the features of the BBB that any given model attempts to reproduce. The DIV-BBB may, for example, become an useful tool for the investigation of long-term effects of drugs or toxins on BBB formation. By using the same model, one can study the dynamics of transendothelial potassium clearance; albeit owing to the aneuronal nature of the DIV-BBB, this approach is limited by the fact that excess potassium must be exogenously applied. Alternatively, the DIV-BBB can be used to study the intimate interactions of astrocytes and endothelial cells or the postnatal development of the blood–brain barrier. It has to be borne in mind, however, that further studies are required to fully account for the different permeability values found between the model and the in situ BBB. In addition, our experiments have thus far concentrated on the study of the physiological properties of the in vitro blood–brain barrier: further experiments are required to fully characterize this system in terms of expression of BBB-specific markers or intracellular enzymes typically encountered in differentiated EC in situ., etc.

In conclusion, we have described the morphological characterization of a novel model of the blood–brain barrier that takes advantage of a state-of-the-art cell culturing

technique, the hollow fiber apparatus. This approach allows for cellular growth under quasi-physiological conditions: these are an essential feature for a successful differentiation of non-BBB EC in vitro or for the maintenance of BBB properties in cultured brain microvascular endothelial cells. Our studies strongly support the hypothesis that glia–endothelial interactions are a fundamental step in the induction of a viable BBB.

Acknowledgements

We would like to thank Claudia Martini for helpful suggestions. This work was supported by NIH Grants NS 51614, 21076, NIEHS ES 07033 (D.J.), NS 30305 (L.E.W.) and NIH M51519 (J.A.N.).

References

[1] H. Davson, M.B. Segal, The blood–brain barrier, in: H. Davson, M.B. Segal (Eds.), Physiology of the CSF and of the blood–brain barrier, CRC, New York, 1995, pp. 49–91.
[2] N.J. Abbott, C.C. Hughes, P.A. Revest, J. Greenwood, Development and characterisation of a rat brain capillary endothelial culture: towards an in vitro blood–brain barrier, J Cell Sci. 103 (1992) 23–37.
[3] A.L. Betz, Sodium transport from blood to brain: inhibition by furosemide and amiloride, J. Neurochem. 41 (1983) 1158–1164.
[4] A.L. Betz, Sodium transport in capillaries isolated from rat brain, J. Neurochem. 41 (1983) 1150–1157.
[5] U. Bickel, T. Yoshikawa, E.M. Landaw, K.F. Faull, W.M. Pardridge, Pharmacologic effects in vivo in brain by vector-mediated peptide drug delivery, Proc. Natl. Acad. Sci. USA 90 (1993) 2618–2622.
[6] M.W. Bradbury, The blood–brain barrier, Exp. Physiol. 78 (1993) 453–472.
[7] M.W. Brightman, T.S. Reese, Junctions between intimately apposed cell membranes in the vertebrate brain, J. Cell. Biol. 40 (1969) 648–677.
[8] A.M. Butt, H.C. Jones, N.J. Abbott, Electrical resistance across the blood–brain barrier in anaesthetized rats: a developmental study, J. Physiol. (Lond.) 429 (1990) 47–62.
[9] P.A. Cancilla, J. Bready, J. Berliner, Brain endothelial-astrocyte interactions, in: W.M. Pardridge (Ed.), The Blood–brain Barrier Cellular and Molecular Biology, Raven, New York, 1993, pp. 25–47.
[10] C. Chesn'e, M.P. Dehouck, P. Jolliet Riant, F. Br'ee, J.P. Tillement, B. Dehouck, J.C. Fruchart, R. Cecchelli, Drug transfer across the blood–brain barrier: comparison of in vitro and in vivo models, Adv. Exp. Med. Biol. 331 (1993) 113–115.
[11] C. Christian, O. Christensen, Electrical resistance of a capillary endothelium, J. Gen. Physiol. 77 (1981) 349–371.
[12] C. Crone, S.P. Olesen, Electrical resistance of brain microvascular endothelium, Brain Res. 241 (1982) 49–55.
[13] L. Dallaier, L. Tremblay, R. Beliveau, Purification and characterization of metabolically active capillaries of the blood–brain barrier, Biochem. J. 276 (1991) 745–752.
[14] H. Davson, W.H. Oldendorf, Transport in the central nervous system, Proc. R. Soc. Med. 60 (1967) 326–328.
[15] H. Davson, M.B. Segal, Blood–brain–CSF interactions, in: H. Davson, M.B. Segal (Eds.), Physiology of the CSF and Blood–brain Barriers, CRC, Boca Raton, FL, 1995, pp. 257–302.
[16] L.E. De Bault, P.A. Cancilla, Gammaglutamyl transpeptidase in isolated brain endothelial cells: induction by glial cells in vitro, Science 207 (1980) 653–655.
[17] M.P. Dehouck, S. Meresse, P. Delorme, J. Fruchart, R. Cecchelli, An easier, reproducible,and mass-production method to study the blood–brain barrier in vitro, J. Neurochem. 54 (1990) 1798–1801.
[18] E.L. Gordon, P.E. Danielsson, T. Nguyen, H.R. Winn, A comparison of primary cultures of rat cerebral microvascular cells to aortic endothelial cells, In Vitro Cell Dev. Biol. 27 (1991) 312–326.
[19] E. Guatteo, K.A. Stanness, D. Janigro, Hyperpolarization-activated currents in cultured rat cortical and spinal cord astrocytes, Glia 16 (1996) 196–209.
[20] D. Janigro, T. Nguyen, E.L. Gordon, H.R. Winn, Physiological properties of ATP-activated cation channels in rat microvascular endothelial cells, Am. J. Physiol. 270 (1996) H1423–H1434.
[21] D. Janigro, K.A. Stanness, T. Nguyen, D.L. Tinklepaugh, H.R. Winn, Possible role of glia in the induction of CNS-like properties in aortic endothelial cells: ATP-activated channels, in: L. Bellardinelli, A. Pelleg (Eds.), Adenosine and Adenine Nucleotides, Nijhoff, Boston, 1995, pp. 85–95.
[22] R.C. Janzer, M.C. Raff, Astrocytes induce blood–brain barrier properties in endothelial cells, Nature 325 (1987) 235–257.
[23] H.C. Jones, R.F. Keep, A.M. Butt, The development of ion regulation at the blood–brain barrier, Prog. Brain Res. 91 (1992) 123–131.
[24] F. Joo, The blood–brain barrier in vitro: Ten years of research on microvessels isolated from brain, Neurochem. Int. 7 (1985) 1–25.
[25] F. Joo, The blood–brain barrier in vitro: the second decade, Neurochem. Int. 23 (1993) 499–521.
[26] F. Joo, A new generation of model systems to study the blood brain barrier: the in vitro approach, Acta Physiol. Hung. 81 (1993) 207–218.
[27] Y.S. Kang, W.M. Pardridge, Use of neutral avidin improves pharmacokinetics and brain delivery of biotin bound to an avidin-monoclonal antibody conjugate, J. Pharmacol. Exp. Ther. 269 (1994) 344–350.
[28] R.A. Knazek, P.M. Gullino, P.O. Kohler, R.L. Dedrick, Cell culture on artificial capillaries: an approach to tissue growth in vitro, Science 178 (1972) 65–67.
[29] J. Laterra, G.W. Goldstein, Brain microvessels and microvascular cells in vitro, in: W.M. Pardridge (Ed.), The Blood–brain Barrier Cellular and Molecular Biology, Raven, 1993, pp. 1–25.
[30] K.J. Lucchesi, R.E. Gosselin, Mechanism of L-glucose, raffinose, and inulin transport across intact blood–brain barriers, Am. J. Physiol. 258 (1990) H695–705.
[31] K.D. McCarthy, J. de Vellis, Preparation of separate astroglial and oligodendroglial cell cultures from rat cerebral tissues, J. Cell. Biol. 85 (1980) 890–899.
[32] A.V. Moses, J.A. Nelson, HIV infection of human brain capillary endothelial cells: implications for AIDS dementia, Adv. Neuroimmunol. 4 (1994) 239–247.
[33] A.V. Moses, S.G. Stenglein, J.G. Strussenberg, K. Wehlry, B. Chesebro, J.A. Nelson, Sequences regulating tropism of HIV type-1 for brain capillary endothelial cells map to a unique region of the viral genome, J. Virol. 70 (1996) 3401–3406.
[34] E.A. Neuwelt, D.L. Goldman, S.A. Dahlborg, J. Crossen, F. Ramsey, S. Roman Goldstein, R. Braziel, B. Dana, Primary CNS lymphoma treated with osmotic blood–brain barrier disruption: prolonged survival and preservation of cognitive function, J. Clin. Oncol. 9 (1991) 1580–1590.
[35] W.H. Oldendorf, Brain uptake of radiolabeled aminoacids, amines, and hexoses after arterial injection, Am. J. Physiol. 221 (1971) 1629–1639.
[36] M.J. Ott, J.L. Olson, B.J. Ballermann, Chronic in vitro flow promotes ultrastructural differentiation of endothelial cells, Endothelium 3 (1995) 21–30.
[37] W.M. Pardridge, J. Boado, Molecular cloning and regulation of gene expression of blood–brain barrier glucose transporter, in: W.M.

Pardridge (Ed.), The Blood–brain Barrier, Raven, New York, 1993, pp. 395–440.
[38] W.M. Pardridge, Y.S. Kang, J.L. Buciak, Transport of human recombinant brain-derived neurotrophic factor (BDNF) through the rat blood–brain barrier in vivo using vector-mediated peptide drug delivery, Pharm. Res. 11 (1994) 738–746.
[39] W.M. Pardridge, D. Triguero, J. Yang, P.A. Cancilla, Comparison of in vitro and in vivo models of drug transcytosis through the blood–brain barrier, J. Pharmacol. Exp. Ther. 253 (1990) 884–891.
[40] M. Pekny, P. Leveen, M. Pekna, C. Eliasson, C. Berthold, B. Westermark, C. Betsholtz, Mice lacking GFAP display astrocytes devoid of intermediate filaments but develop and reproduce normally, EMBO J. 14 (1995) 1590–1598.
[41] T.S. Reese, L.J. Karnovsky, Structure localization of a blood brain barrier to exogenous peroxidase, J. Cell Biol. 34 (1967) 207–217.
[42] W. Risau, Induction of blood–brain barrier endothelial differentiation, Ann. NY Acad. Sci. 633 (1991) 405–419.
[43] P.J. Robinson, S.I. Rapoport, Glucose transport and metabolism in the brain, Am. J. Physiol. 250 (1986) R127–36.
[44] L.L. Rubin, D.E. Hall, S. Porter, K. Barbu, C. Cannon, H.C. Horner, M. Janatpour, C.W. Liaw, K. Manning, J. Morales, A cell culture model of the blood–brain barrier, J. Cell. Biol. 115 (1991) 1725–1735.
[45] A. Selig, R. Gottschlich, R.M. Devant, A method to determine the ability of drugs to diffuse through the blood–brain barrier, Proc. Natl. Acad. Sci. USA 91 (1994) 68–72.
[46] K.A. Stanness, E. Guatteo, D. Janigro, A dynamic model of the blood–brain barrier in vitro, Neurotoxicology 17 (1996) 481–496.
[47] P.A. Stewart, M.J. Wiley, Developing nervous system induces formation of blood–brain barrier characteristics in invading endothelial cells: a study using quail-chick transplantation chimeras, Dev. Biol. 84 (1981) 183–192.
[48] W. Stummer, R.F. Keep, A.L. Betz, Rubidium entry into brain and cerebrospinal fluid during acute and chronic alterations in plasma potassium, Am. J. Physiol. 266 (1994) H2239–H2246.
[49] U. Tontsch, H.C. Bauer, Glial cells and neurons induce blood–brain barrier related enzymes in cultured cerebral endothelial cells, Brain Res. 6 (1991) 271–283.
[50] B. Veronesi, In vitro screening batteries for neurotoxicants, Neurotoxicology 13 (1992) 185–195.
[51] A.W. Vorbrodt, Morphological evidence of the functional polarization of brain microvascular endothelium, in: W.M. Pardridge (Ed.), The Blood–brain Barrier Cellular and Molecular Biology, Raven, New York, 1993, pp. 137–164.
[52] J.G. Zhou, J.R. Meno, S.S. Hsu, H.R. Winn, Effects of theophylline and cyclohexyladenosine on brain injury following normo- and hyperglycemic ischemia: a histopathologic study in the rat, J. Cereb. Blood Flow Metab. 14 (1994) 166–173.